Supporting Information

Optimized Lithium Deposition on Ag Nanoparticles-Embedded TiO_2 Microspheres: A Facile Spray Pyrolysis Approach for Enhanced Lithium Metal Anode

Jae Wook Kang[†,a], Jae Hun Choi[†,a], Jung-Kul Lee*[,b], and Yun Chan Kang*[,a]

[a] Department of Materials Science and Engineering, Korea University, Anam-Dong, Seongbuk-Gu, Seoul 136-713, Republic of Korea
[b] Department of Chemical Engineering, Konkuk University, Hwayang-Dong, Gwangjin-Gu, Seoul 143-701, Republic of Korea

[†] These two authors contributed equally to this work.

* Corresponding author:
E-mail address: yckang@korea.ac.kr; (Yun Chan Kang), jkrhee@konkuk.ac.kr; (Jung-Kul Lee)

Experimental Section

Material Characterization

The microstructure and morphology of the samples were examined using scanning electron microscopy (SEM, TESCAN, VEGA3) and transmission electron microscopy (TEM, JEOL, JM-2100F). The crystallographic analysis of the samples was conducted via X-ray diffraction (XRD) employing Cu-Kα radiation ($\lambda = 0.154$ nm) on the X-ray diffractometer (X's pert PRO MPD) at the Korea Basic Science Institute (Daegu). The analysis of surface chemical states in the samples was conducted via X-ray photoelectron spectroscopy (XPS) (K-Alpha; Thermo Scientific) with an Al Kα X-ray source. The specific surface area and porosities of the sample were estimated by using N_2 gas based on the Brunauer-Emmett-Teller (BET) method. Lithium deposited electrodes were analyzed by the focused ion beam-scanning transmission electron microscope (FIB-STEM, Helios G4, FEI) to investigate the lithium deposition mechanism in the sample. Platinum was deposited to protect the initial atomic layers of the surface with a few nanometers, and all FIB cuts were performed using 3 kV/230 pA conditions for the rough raster, with a final ionic polishing step being carried out via a 30 kV/80 pA ion beam.

Electrochemical measurement

To test the electrochemical properties of the samples, CR2032 coin-type cells were assembled in an Ar-filled glove box. The slurry was prepared by mixing the sample powders and polyvinylidene fluoride (PVDF) at a mass ratio of 9:1 in N-methyl-2-pyrrolidone (NMP) as the solvent. The slurry was coated on the Cu foil using a doctor blade and completely dried in a vacuum oven at 60 ^{o}C overnight. The mass loading of the anode electrode was 5.8 mg cm^{-2}. To test the asymmetrical cell and symmetrical cell, the electrolyte used was 1.0 M lithium bis(trifluoromethane)sulfonamide (LiTFSI) in a mixture of 1,2-dimethoxyethane (DME) and 1,3-dioxolane (DOL) (1:1 in volume) with 0.3 M $LiNO_3$. During the initial two cycles of the asymmetrical cell tests, the cells were cycled in the potential range of 0-1.0 V at 1.0 mA cm^{-2} to stabilize the SEI and remove surface contaminants. For the symmetrical cell and full cell tests, lithium was deposited on the working electrodes with a capacity of 5.0 mAh cm^{-2} at a current density of 1.0 mA cm^{-2}. In full cells, NCM 811 cathodes were obtained by mixing NCM 811 (80 wt%), PVDF (10 wt%), and Super-P (10 wt%) conductive agent in NMP solvent. Subsequently, the uniform slurry was pasted on Al foil and then dried at 60 ^{o}C in a vacuum oven overnight. The mass loading of NCM 811 was 6.1 mg cm^{-2}. The electrolyte used for full cells was 1 M $LiPF_6$ in ethylene carbonate (EC) and ethyl methyl carbonate (EMC) (3:7 in volume) with 2 wt% fluoroethylene carbonate (FEC). Based on the theoretical capacity of NCM 811(200 mAh g^{-1}), the capacity of the cathode can be calculated into 1.2 mAh cm^{-2}. In addition, as the capacity of 5.0 mAh cm^{-2} of lithium was deposited on the anode electrode, the N/P ratio of the full cells was calculated to be 4.1.

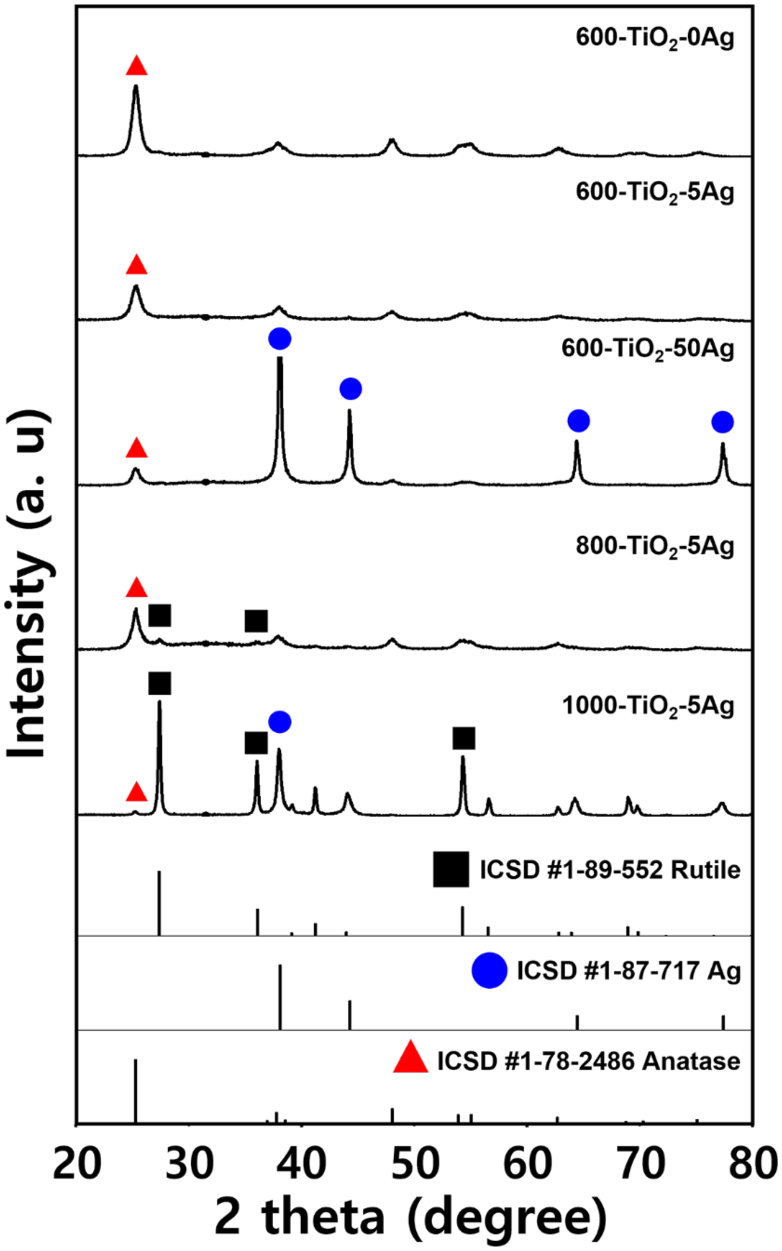

Figure S1. XRD patterns of TiO_2-Ag composite microspheres.

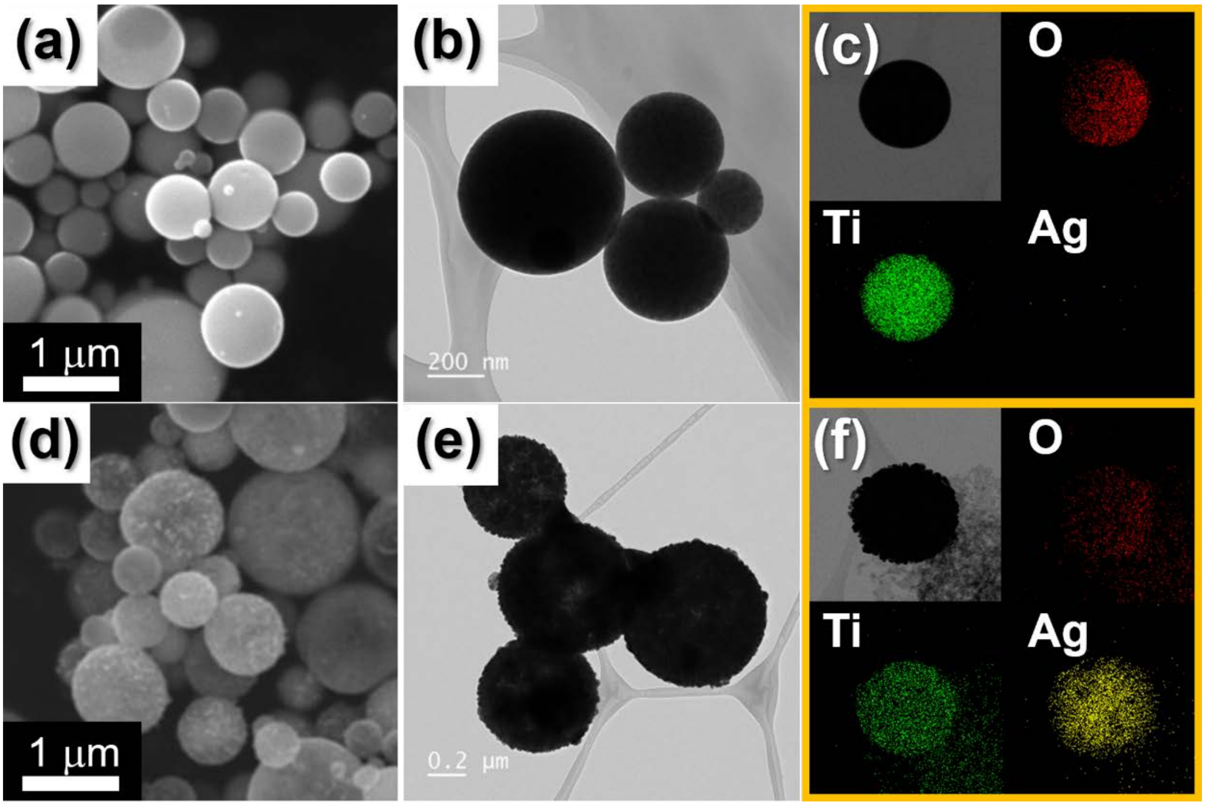

Figure S2. Morphologies of (a-c) 600-TiO_2-1Ag and (d-f) 600-TiO_2-50Ag microspheres: (a, d) SEM images, (b, e) TEM images, and (c, f) elemental mapping images.

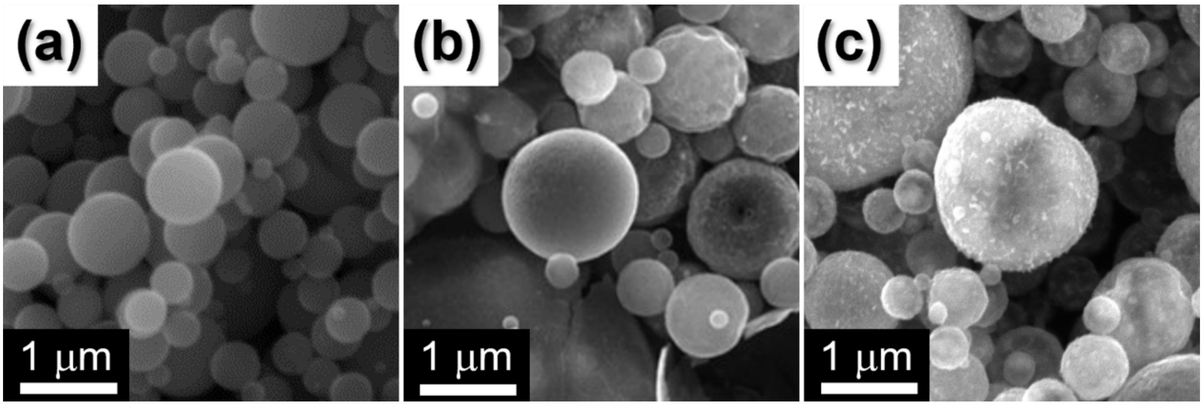

Figure S3. SEM images TiO_2-Ag composite microspheres: (a) 600-TiO_2-0Ag, (b) 800-TiO_2-5Ag, and (c) 1000-TiO_2-5Ag.

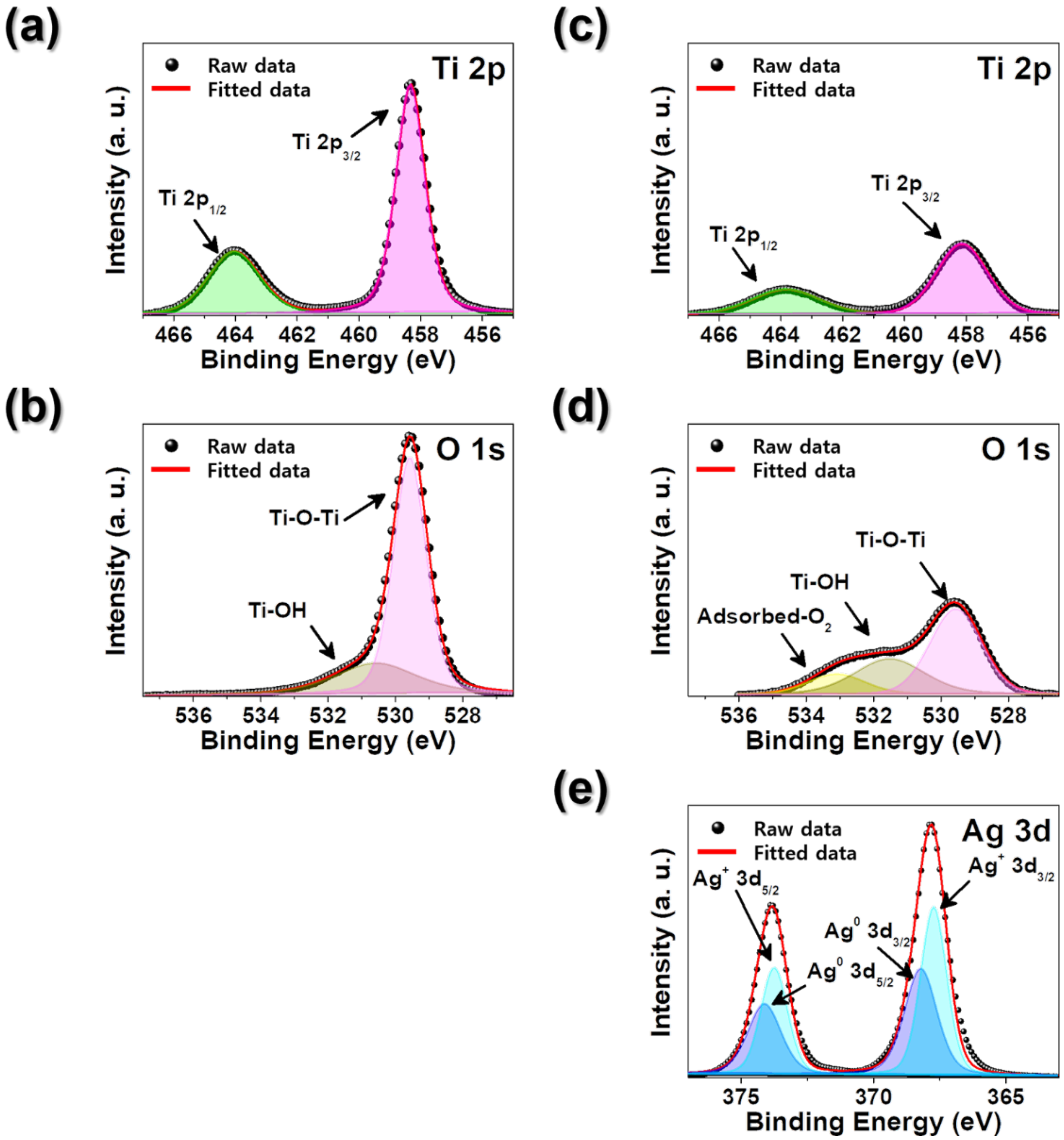

Figure S4. XPS spectra of (a, b) 600-TiO2-0Ag and (c-e) 600-TiO2-50Ag microspheres: (a, c) Ti 2p, (b, d) O 1s, and (e) Ag 3d.

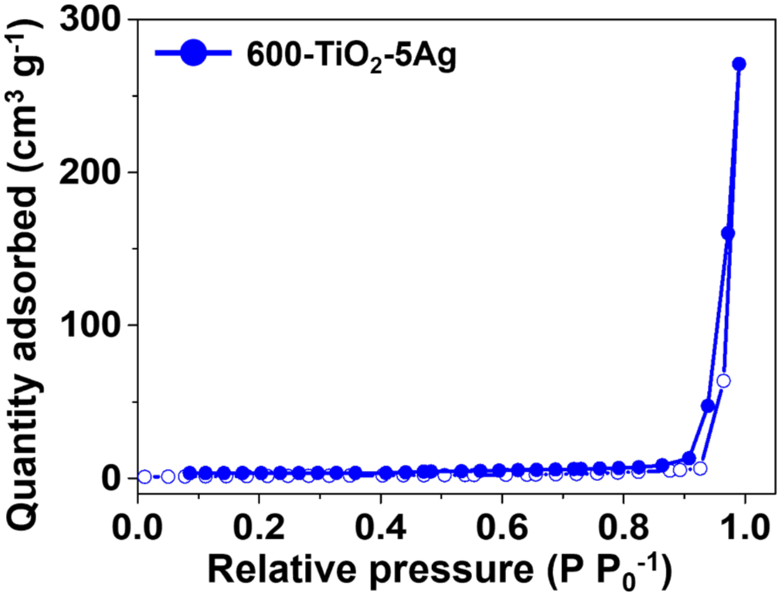

Figure S5. N_2 adsorption and desorption isotherm of 600-TiO_2-5Ag microspheres.

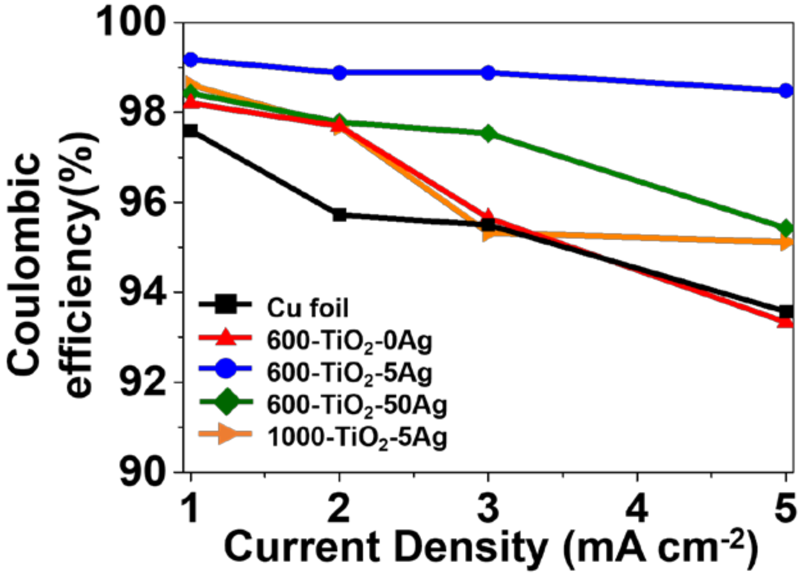

Figure S6. The average CEs during the cycling of the bare Cu foil, 600-TiO_2-0/5/50Ag, and 1000-TiO_2-5Ag as the working electrode, the asymmetrical cell tests were conducted at the current density of 1.0, 2.0, 3.0, and 5.0 mA cm^{-2} with the capacity of 1.0 mAh cm^{-2}.

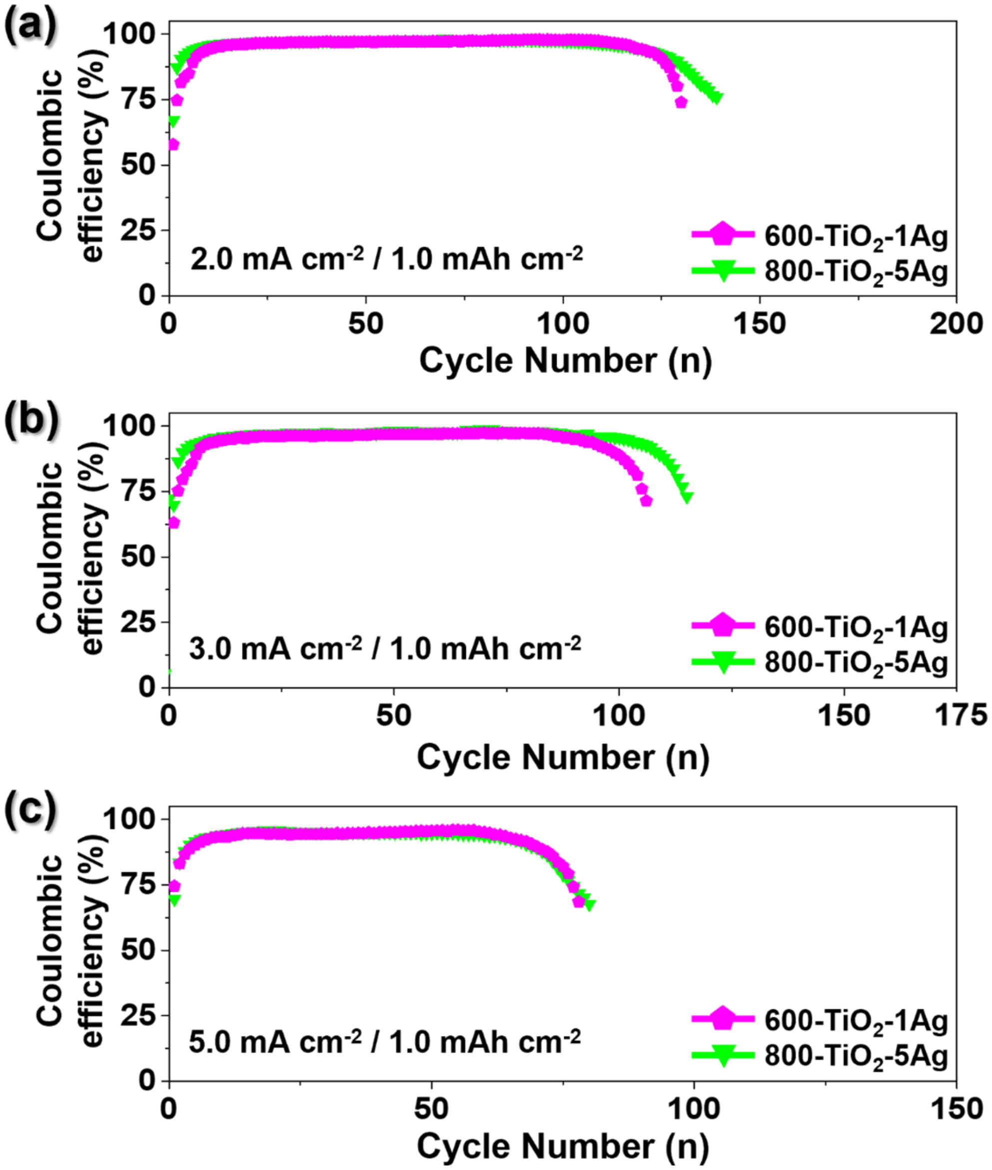

Figure S7. CEs of 600-TiO_2-1Ag and 800-TiO_2-5Ag microspheres when cycled at different current densities with a cycling capacity of 1.0 mAh cm^{-2}: (a) 2.0 mA cm^{-2}, (b) 3.0 mA cm^{-2}, and (c) 5.0 mA cm^{-2}.

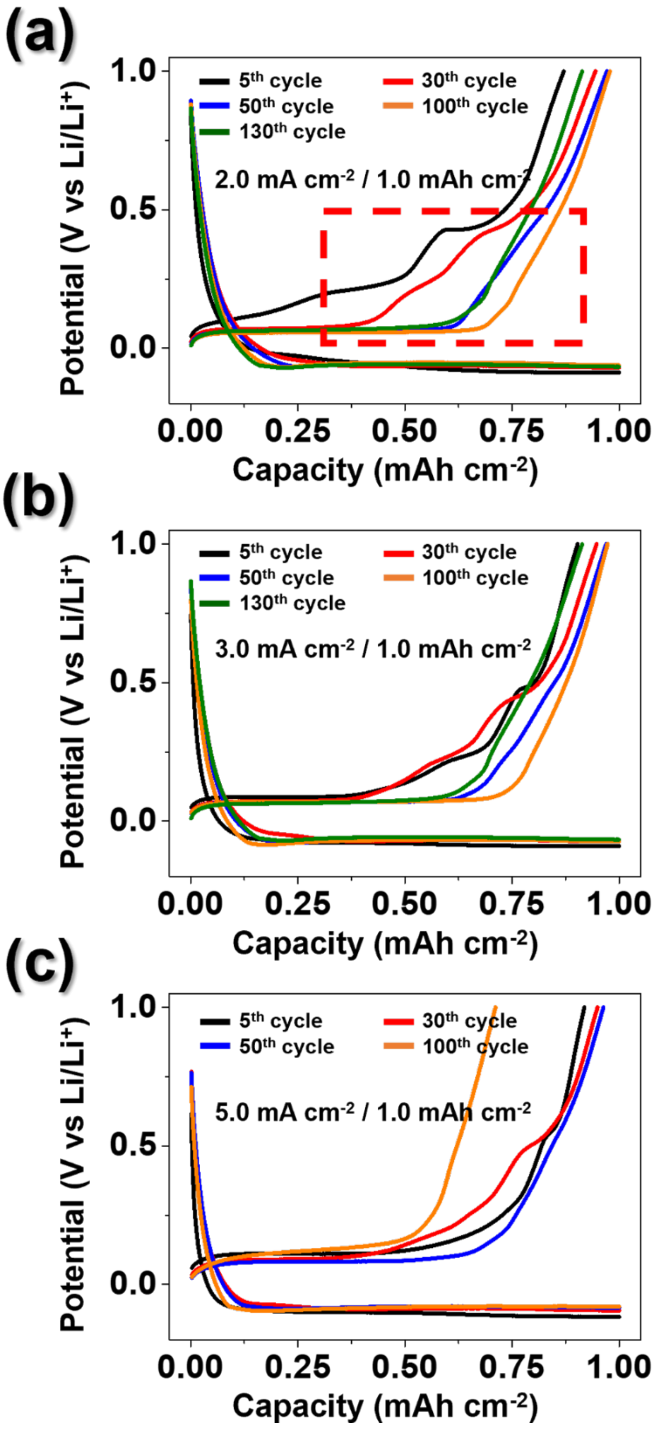

Figure S8. Voltage profiles of 600-TiO_2-50Ag microspheres in asymmetrical cell tests, cycled with a cycling capacity of 1.0 mAh cm^{-2} at current densities of (a) 2.0 mA cm^{-2}, (b) 3.0 mA cm^{-2}, and (c) 5.0 mA cm^{-2}.

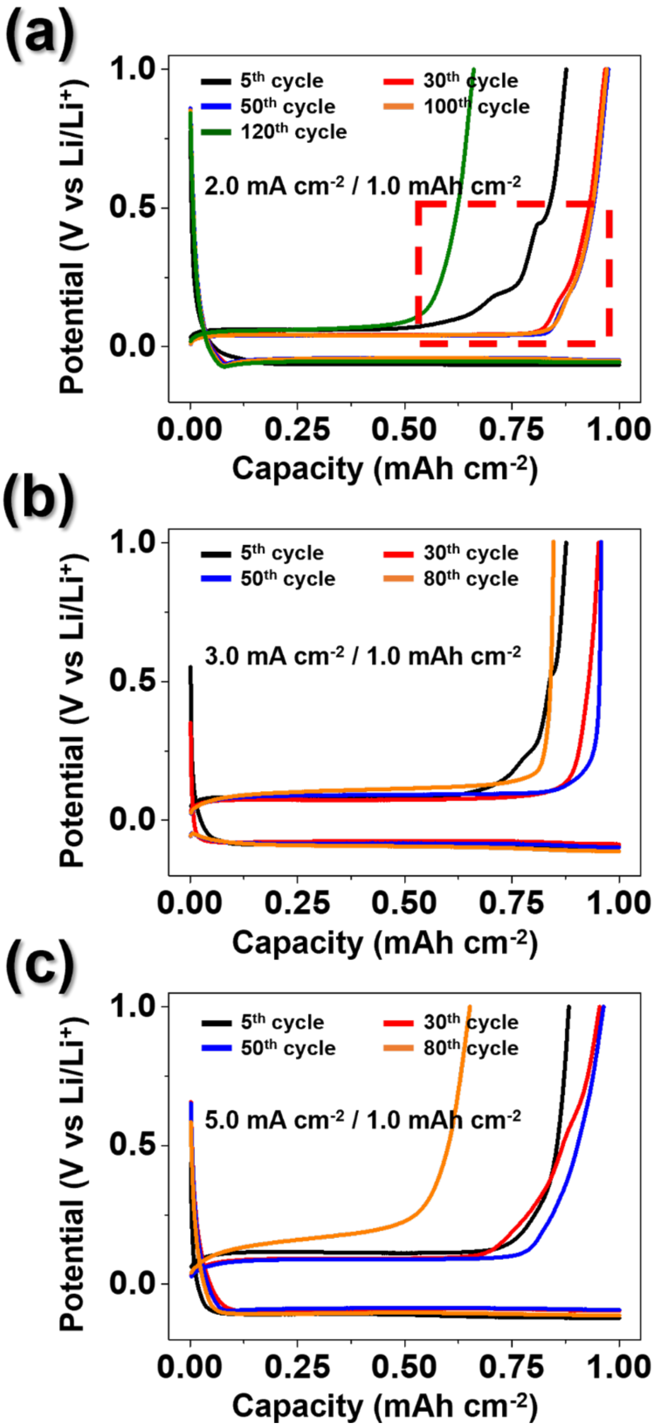

Figure S9. Voltage profiles of 1000-TiO_2-5Ag microspheres in asymmetrical cell tests, cycled with a cycling capacity of 1.0 mAh cm^{-2} at current densities of (a) 2.0 mA cm^{-2}, (b) 3.0 mA cm^{-2}, and (c) 5.0 mA cm^{-2}.

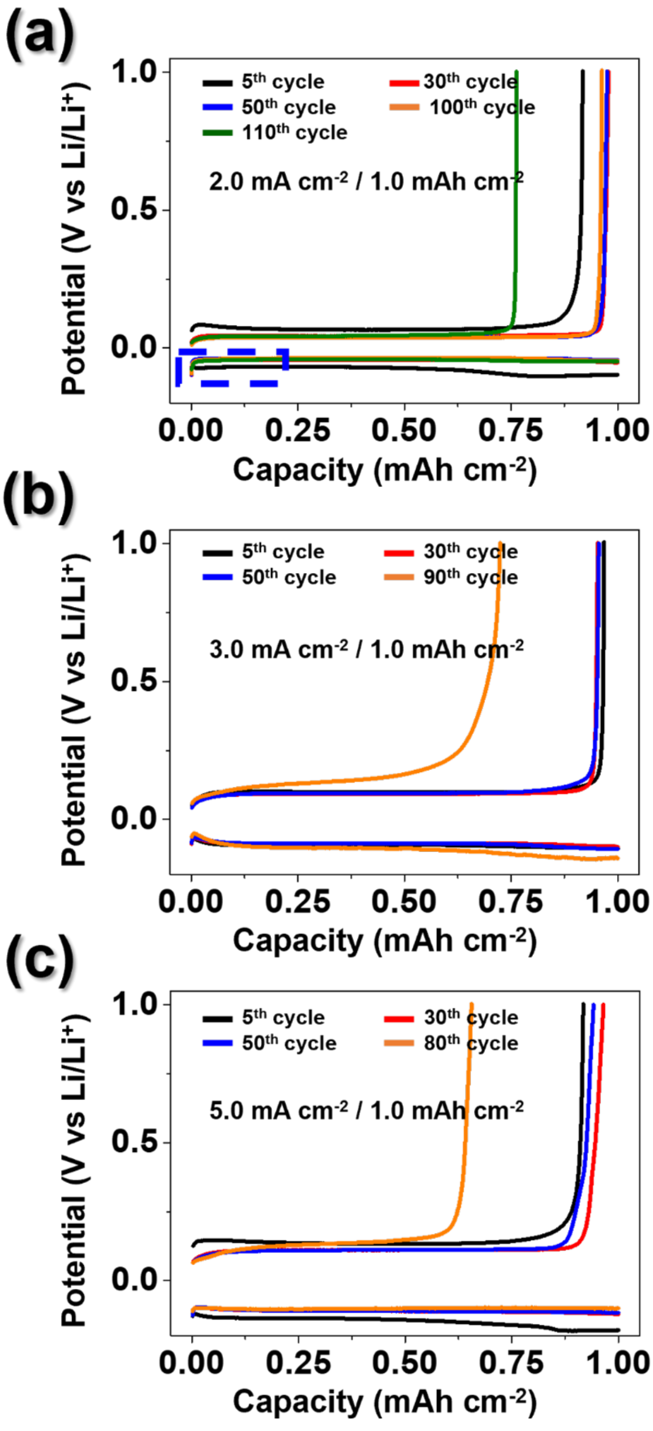

Figure S10. Voltage profiles of 600-TiO$_2$-0Ag microspheres in asymmetrical cell tests, cycled with a cycling capacity of 1.0 mAh cm^{-2} at current densities of (a) 2.0 mA cm^{-2}, (b) 3.0 mA cm^{-2}, and (c) 5.0 mA cm^{-2}.

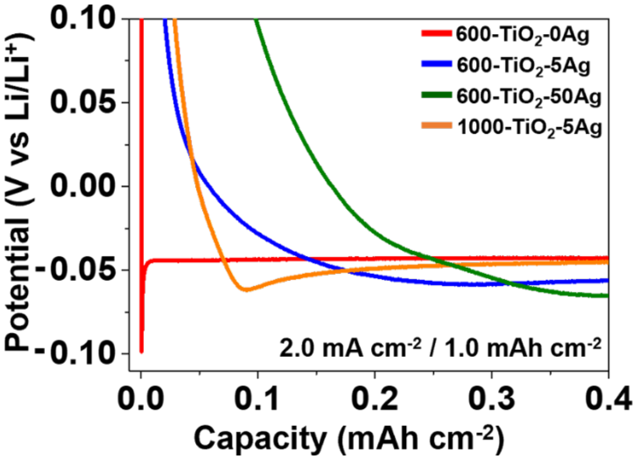

Figure S11. Nucleation overpotential of TiO$_2$-Ag microspheres at a current density of 1.0 mA cm^{-2} obtained after 30 cycles.

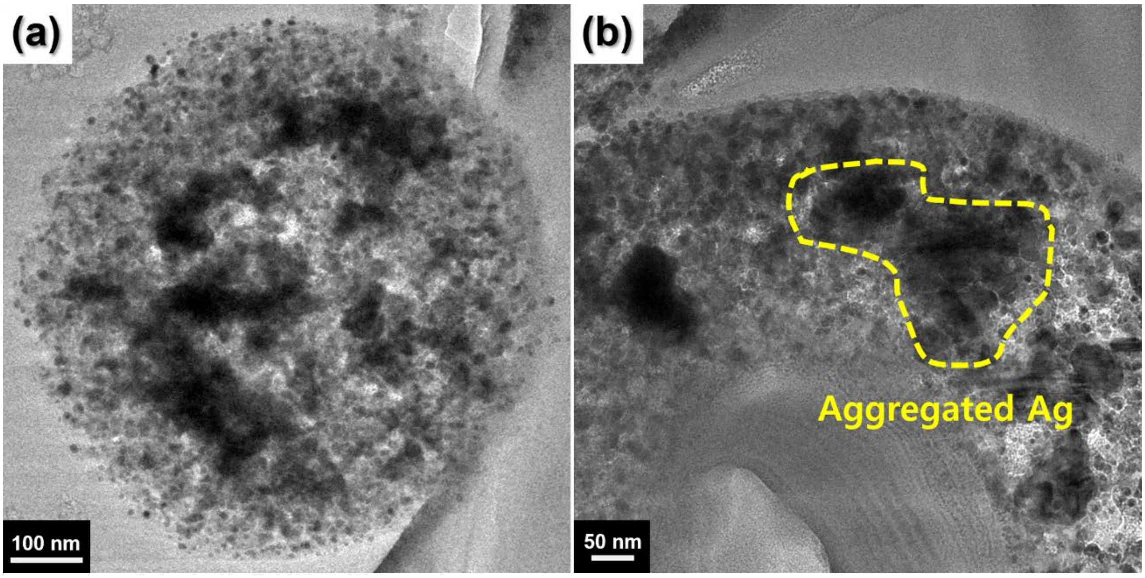

Figure S12. TEM images of 600-TiO_2-50Ag microspheres before lithium deposition.

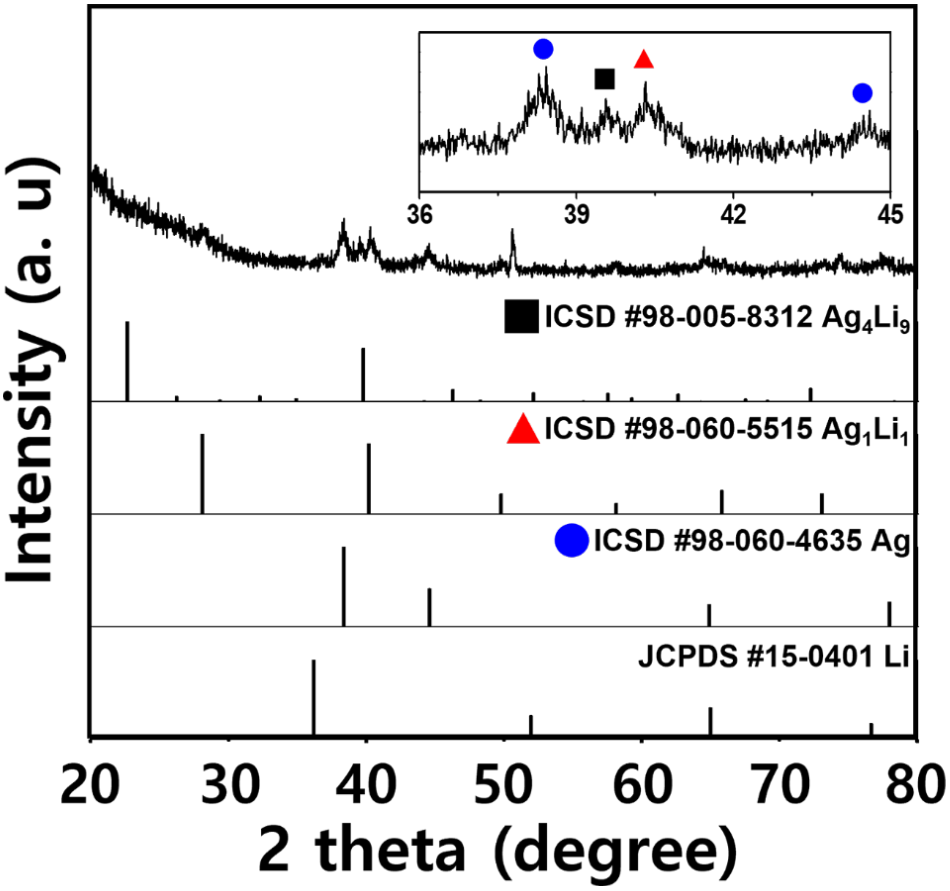

Figure S13. XRD pattern of the 600-TiO_2-50Ag electrode after depositing 1.0 mAh cm^{-2} of lithium.

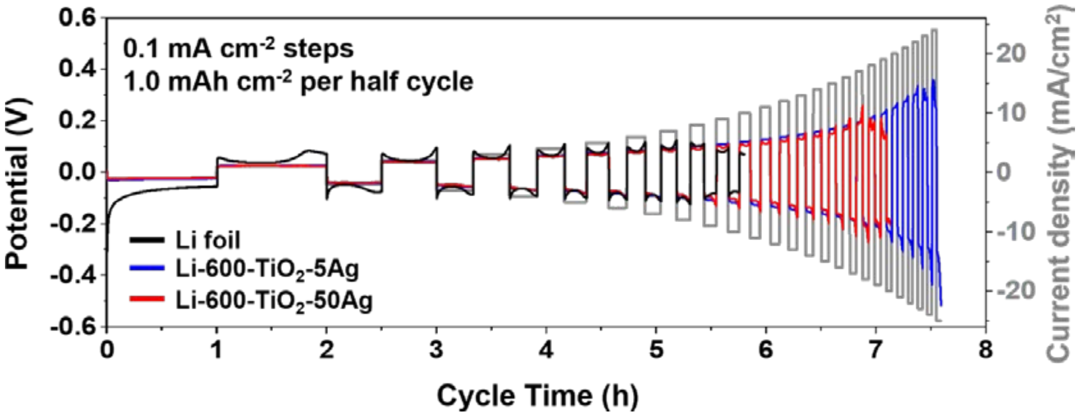

Figure S14. CCD measurements of bare Li foil, Li-600-TiO$_2$-5Ag, and Li-600-TiO$_2$-50Ag symmetrical cells.

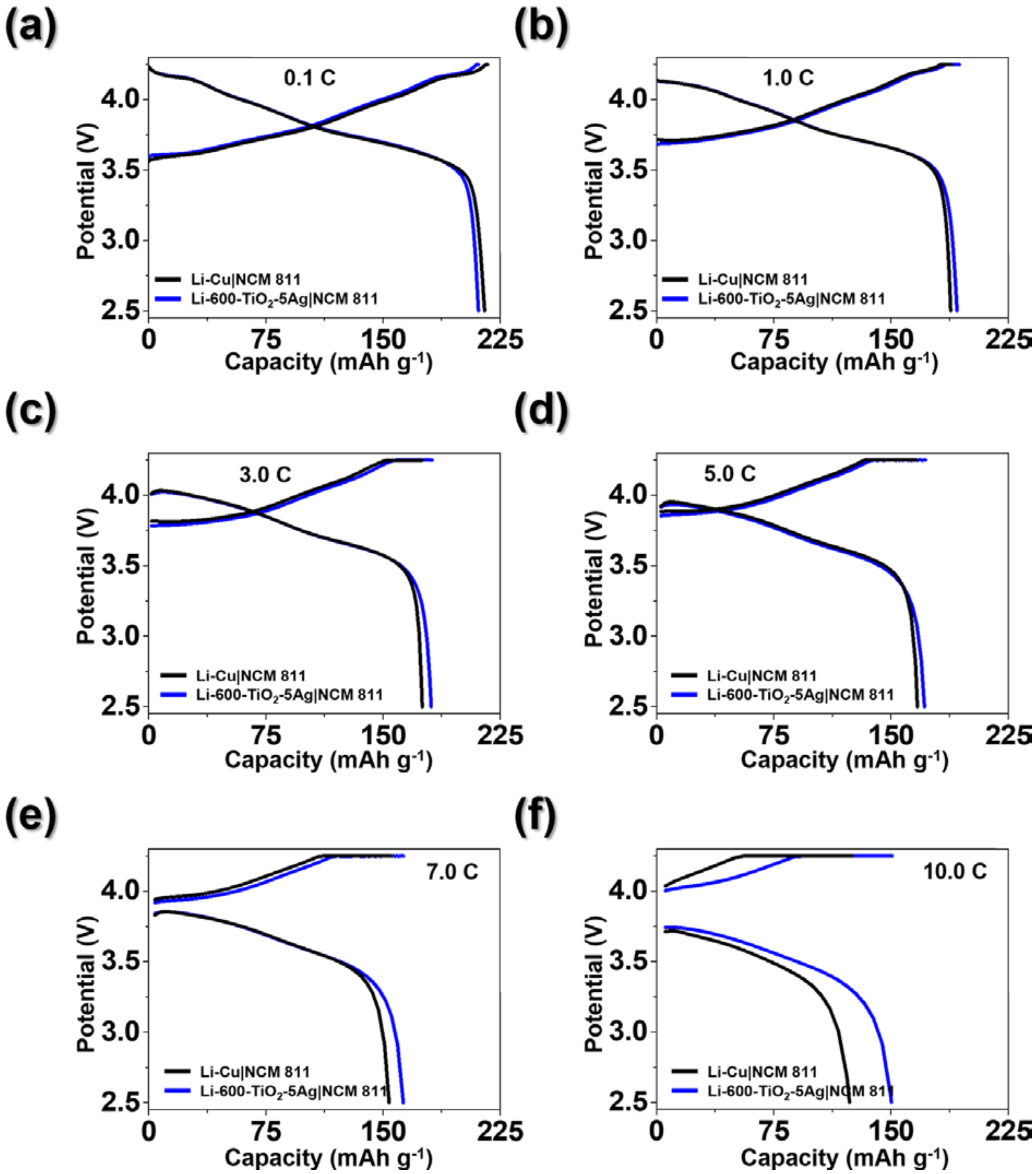

Figure S15. Voltage profiles of the Li-Cu|NCM 811 and Li-600-TiO_2-5Ag|NCM 811 full cells at the current density of (a) 0.1 C, (b) 1.0 C, (c) 3.0 C, (d) 5.0 C, (e) 7.0 C, and (f) 10.0 C.